



Title	In-situ Observation of martensite transformation and retained austenite in supermartensitic stainless steel
Author(s)	Zhang, Shuoyuan; Terasaki, Hidenori; Komizo, Yu-ichi
Citation	Transactions of JWRI. 2010, 39(2), p. 115-117
Version Type	VoR
URL	<a href="https://doi.org/10.18910/9053">https://doi.org/10.18910/9053</a>
rights	
Note	

*The University of Osaka Institutional Knowledge Archive : OUKA*

<https://ir.library.osaka-u.ac.jp/>

The University of Osaka

# In-situ Observation of martensite transformation and retained austenite in supermartensitic stainless steel<sup>†</sup>

ZHANG Shuoyuan<sup>\*</sup>, TERASAKI Hidenori<sup>\*\*</sup> and KOMIZO Yu-ichi<sup>\*\*\*</sup>

**KEY WORDS:** (Martensite Transformation) (Retained Austenite) (In situ Observation) (X-ray Diffraction) (Synchrotron Radiation)

## 1. Introduction

Supermartensitic steel (14CrNiMo) is a candidate as a weld metal for joining of ultra-high strength steels. For preventing the cold cracking problem, the austenite phase is effective due to its nature of hydrogen absorption and the existing of austenite phases increases toughness of weld metal. Moreover, the residual stress can be decreased by introducing the martensite transformation expansion. On the other hand, too much retained austenite could decrease the strength of Supermartensitic steel. Hence, determination of the retained austenite is important in Supermartensitic steel.

In this research, martensite transformation of supermartensitic steel during cooling was observed in-situ by using high temperature laser scanning confocal microscopy and X-ray diffraction by Synchrotron radiation. The ultra-bright, directional and quasi monochromatic natures of the beam were suitable as the probe for our purpose.

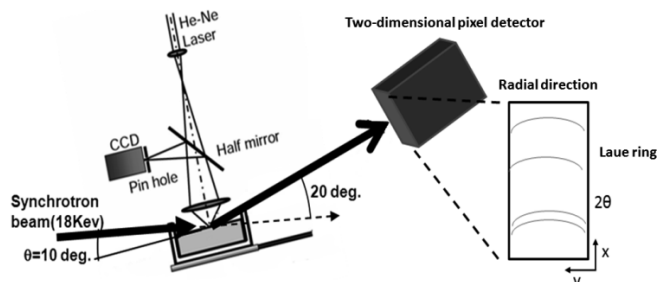


**Fig.1** Schematic illustration of in-situ observations experiments system.

## 2. Experimental

In this study, for analysis of behavior of retained austenite in martensite transformation, supermartensitic steel was prepared with different nickel contents. The Ms of supermartensitic steel of 14Cr9Ni was low, and a large amount of retained austenite remained in the specimen cooled down to room temperature. After the specimens were heated from room temperature to 1000 degree C and cooled down to room temperature. The Martensite

transformation of Supermartensitic steel during cooling was observed in-situ by using high temperature laser scanning confocal microscopy and X-ray diffraction by Synchrotron radiation.

The schematic illustration of the In-situ observation system is shown in **Figure 1**[1]. The In-situ observation system consists of High-Temperature Laser Scanning Confocal Microscopy (HLSCM) system[2, 3] and Time-Resolved X-ray Diffraction (TRXRD) system. The High-Temperature Laser Scanning Confocal Microscopy (HLSCM) system was used for direct observation of the martensite transformation during the thermal cycles.

The Time-Resolved X-ray Diffraction (TRXRD) systems were performed on the BL46XU beam line with the undulator of third generation synchrotron radiation source, Spring-8, with the approval of the Japan Synchrotron Radiation Research Institute (Hyogo, Japan). This research, gives a time resolution of 0.2 seconds by using PILATUS 100K detector. The diffraction intensities at various  $2\theta$  positions were monitored continuously and in real time using a detector covering a  $2\theta$  range of approximately from  $12^\circ$  to  $28^\circ$ . In general, two body-centered cubic (bcc) martensite peaks [110 and 200] and two face-centered cubic (fcc) austenite peaks [111 and 200] were identified.

## 3. Results and Discussion

**Figure 2** shows the in-situ observation of morphological development and the diffraction patterns recorded on the pixel detector for the sample 14Cr5Ni. Fig. 2(a) to (c) correspond to the heating process from the room temperature, while Fig.2(d) to (f) show the martensite transformation during cooling process. There were four peaks visible in the diffraction patterns, representing  $\alpha(110)$ ,  $\alpha(200)$ ,  $\gamma(111)$  and  $\gamma(200)$ . The materials consists of  $\alpha'$ -martensite,  $\alpha(110)$  and  $\alpha(200)$ , at room temperature shown in Fig.2(a). As shown in Fig.2(b),  $\gamma(111)$  and  $\gamma(200)$  reflections were first identified at 758 degree C, indicating the initiation of transformation from  $\alpha'$ - martensite to  $\gamma$ -austenite. Furthermore  $\alpha(110)$  and  $\alpha(200)$  reflections disappeared at 907 degree C in Fig.2(c) , which represents the complete transformation to austenite.

<sup>†</sup> Received on 30 September 2010

<sup>\*</sup> Graduate School of Engineering, Osaka University, Osaka, Japan

<sup>\*\*</sup> Joining and Welding Research Institute, Osaka University, Osaka, Japan

Transactions of JWRI is published by Joining and Welding Research Institute, Osaka University, Ibaraki, Osaka 567-0047, Japan

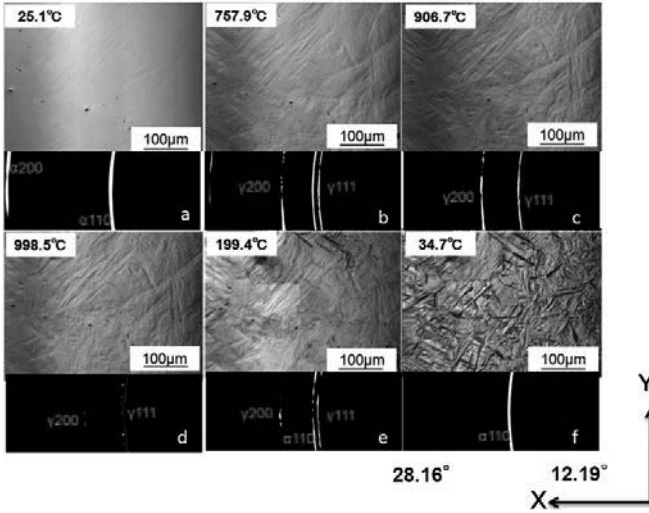


**Fig. 2** Overview of the In-situ Observation results for martensite transformation for 14Cr5Ni Using high temperature laser scanning confocal microscopy and Synchrotron Radiation X-ray diffraction. The x-y axis corresponded to that in Fig.1.

Fig.2(d) shows that due mainly to the variation of the  $\gamma$ -austenite reflections from a ring pattern to a spot pattern, because the austenite grain sizes become larger. As shown in Fig.2(e),  $\alpha(110)$  reflection first appeared at 199 degree C, which corresponds to the beginning of transformation from  $\gamma$ -austenite to  $\alpha$ -martensite. Subsequently, as the transformation proceeded,  $\gamma(111)$  and  $\gamma(200)$  reflections disappear at 35 degree C, as shown in Fig.2(f). This means the transformation of  $\gamma$ -austenite to  $\alpha$ -martensite is fully completed.

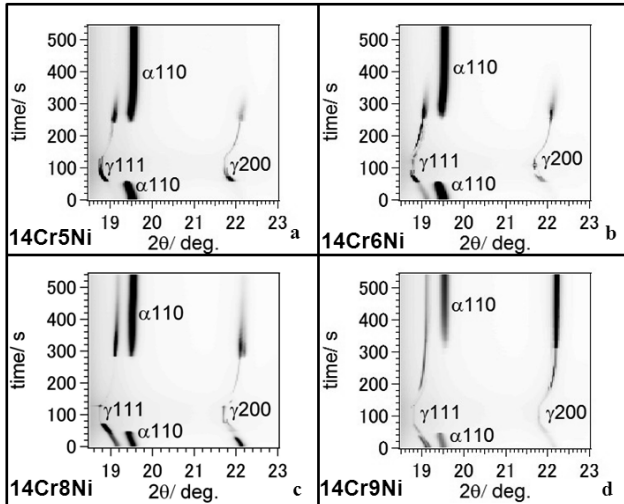


**Fig. 3** X-ray diffraction sequence for the first 0s to final 540s for all the samples, 14Cr5Ni, 14Cr6Ni, 14Cr8Ni, and 14Cr9Ni. The black corresponds to the peak highest intensities and white the lowest.

**Figures 3(a) to (d)** show the  $2\theta$  values of the diffraction peaks plotted as a function of time for all the samples, 14Cr5Ni, 14Cr6Ni, 14Cr8Ni, and 14Cr9Ni. It was shown

for all the samples that  $2\theta$  decreases with increasing time, during heating process. On the cooling process,  $2\theta$  increased with increasing time. It was also shown in the figure that as the martensite transformation proceeds, in the higher full width at half maximum (FWHM) and the intensity of  $\gamma(111)$  and  $\gamma(200)$  reflections becomes stronger.

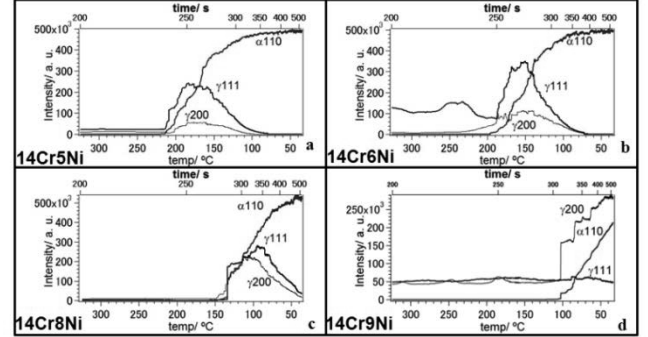


**Fig. 4** Intensities of  $\gamma(111)$ ,  $\gamma(200)$  and  $\alpha(110)$  for the last 340s of the cooling to room temperature.

**Figures 4(a) to (d)** show the intensity of  $\alpha(110)$ ,  $\gamma(111)$  and  $\gamma(200)$  as a function of time and temperature for all the samples during cooling process. As the martensite transformation proceeded, the intensity of  $\alpha(110)$  increase with increasing time and decreasing temperature. It is interesting to note that simultaneously the intensity of  $\gamma(111)$  and  $\gamma(200)$  increased with increasing time and decreasing temperature for the first three samples. Subsequently, the intensity of  $\gamma(111)$  and  $\gamma(200)$  decreased with increasing time and decreasing temperature. In Fig.4(d), the intensity of  $\gamma(111)$  and  $\gamma(200)$  increased with increasing time and decreasing temperature until the room temperature. A lot of retained austenite has been observed in this sample. In our previous paper[4], EBSD results showed that in this sample twin deformation has been observed and the austenite grain size becomes smaller.

It is generally accepted that ideally perfect crystal and powder crystal have minimum and maximum diffracting power respectively, due to the effect of distinction. Thus, at the initiation of martensite transformation, the intensity of all the samples increases, mainly because the introduction of the metal defects in the parent austenite increased the diffracting power. The intensity of the austenite increases with increasing metal defects, although the content of austenite decreases. The content of austenite decreases as the transformation proceeds. The effect of the intensity of austenite becomes lower due to increasing diffracting power by introduction of the metal defects in the austenite, as a result of decrease intensity of austenite.

#### 4. Conclusions

Martensite transformation of supermartensitic steel was observed in-situ by using high temperature laser scanning confocal microscopy and X-ray diffraction by Synchrotron radiation. The main conclusions obtained are as follows:

- (1) The reflection of austenite changes from a spot pattern to a ring pattern after martensite

transformation.

- (2) Both the higher full width at half maximum (FWHM) and intensity increased due to the effect of martensite transformation.
- (3) At the initiation of martensite transformation, the intensity of austenite increased due to increasing diffracting power by introduction of the metal defects in the austenite.

#### Acknowledgements

This study was carried out as a part of research activities of “Fundamental Studies on Technologies for Steel Materials with Enhanced Strength and Functions” by Consortium of JRCM (The Japan Research and Development Center of Metals). Financial support from

NEDO (New Energy and Industrial Technology Development Organization) is gratefully acknowledged. The synchrotron radiation experiments were performed at the BL46XU in the SPring-8 with the approval of the Japan Synchrotron Radiation Research Institute (JASRI) (Proposal No. 2008A1959, 2008B2135 & 2009A1944).

#### References

- [1]Y. Komizo and H. Terasaki: Sci. Technol. Weld. Join.,(2011) in press.
- [2]H. Terasaki and Y. Komizo: Sci. Technol. Weld. Join.,5(2006) 11, pp. 561-566.
- [3]Y. Komizo, et al.: Weld. World,5-6(2008) 52, pp. 56-63.
- [4]S. Zhang, Y. Komizo, and H. Terasaki: Tetsu-To-Hagane,2(2010) 96, pp. 8-13.